Vorticity organization in the outer layer of turbulent channels with disturbed walls

OSCAR FLORES[1], JAVIER JIMÉNEZ[1,2] AND JUAN C. DEL ÁLAMO[3]

[1]School of Aeronautics, Universidad Politécnica de Madrid, 28040 Madrid, Spain
[2]Center for Turbulence Research, Stanford University, Stanford, CA 94305, USA
[3]MAE Department, University of California San Diego, La Jolla, CA 92093, USA

The vortex clusters in the turbulent outer region of rough- and smooth-walled channels, and their associated velocity structures, are compared using data from numerical experiments at friction Reynolds numbers $Re_\tau \leqslant 674$. The results indicate that the roughness of the wall does not affect their properties, particularly the existence of wall-detached and wall-attached populations, and the self-similar size distribution of the latter. The average flow field conditioned to the attached clusters reveals similar conical structures of low streamwise velocity for the rough- and smooth-walled cases, which eventually grow into the global modes previously identified from spectral analysis. We conclude that the vortex clusters of the turbulent outer region either originate away from the wall, or quickly forget their origin, in agreement with Townsend's similarity hypothesis.

1. Introduction

Turbulent wall flows are a challenging research subject with applications ranging from drag reduction to atmospheric dispersion. The analysis of how their outer layers may be influenced by the structures of the near-wall region is particularly useful, because the latter are altered by the hydraulically rough surfaces often found in engineering and geophysical flows, and because flow control strategies are usually implemented through actuators located at the wall.

It has long been proposed that the inner–outer interactions are due to vortex loops connecting the two layers (see the review by Robinson 1991*a*). The best-known theoretical models are variations of the vortex hierarchies proposed by Perry & Chong (1982) and Perry, Henbest & Chong 1986, loosely based on Townsend's (1976, pp. 150–162) attached-eddy hypothesis. Although those models were initially constructed from abstract eddies, with larger elements emerging from smaller ones through unspecified processes, they eventually evolved into collections of lambda-vortices growing from the wall. Such objects have been observed in low-Reynolds-number numerical simulations (Robinson 1991*b*; Blackburn, Mansour & Cantwell 1996; Chong *et al.* 1998), and in experiments with relatively coarse resolutions (Adrian, Meinhart & Tomkins 2000; Ganapathisubramani, Longmire & Marusic 2003). The resulting picture is of packets of hairpin vortices growing from the wall into the outer region through self-induction, regeneration and mergers, generating long ramps of low streamwise velocity.

A less organized model was proposed by del Alamo *et al.* (2006) (hereafter AJZM06) after analysing vortex clusters in numerical channels at friction Reynolds numbers

$Re_\tau \leqslant 1900$. Those clusters share many of the properties of the large-scale eddies of the theoretical models of vortex forests, but they are 'bags' of vortices in which individual hairpins are difficult to identify. The clusters separate naturally into wall-attached and wall-detached families, and the attached ones have sizes and dimensions similar to the hairpin packets in Ganapathisubramani *et al.* (2003) and Tomkins & Adrian (2003). The average velocity field conditioned to an attached cluster contains a lambda-vortex with a wall-normal velocity ejection between its legs. Tanahashi *et al.* (2004) also observed that the large scales in a channel at $Re_\tau = 800$ were formed by vortex tangles, although they noted that the dominant vortex orientation is consistent with hairpin legs (but with fewer heads) even far from the wall.

The origin and evolution of the vortex packets, whether organized or not, remains elusive, specially regarding how they move away from the wall. Zhou *et al.* (1999) described how a hairpin packet could be created from an initial lambda-vortex in a laminar channel with a turbulent mean profile, but neglected the background fluctuations of real turbulent flows, which might alter significantly the process by shortening the lifetimes and lowering the intensities of the vortices. Moreover, their hairpins moved only moderately far from the wall. AJZM06, showed that the lifetimes of the attached clusters are too short to have grown from the wall to their observed heights, and suggested that they originate at all heights, sizes and wall distances.

The origin of the vortex packets of the outer layer has implications for flows over rough walls. The classical theory states that the outer region is independent of the wall roughness and of the fluid viscosity ν, as long as the Reynolds number is high enough, and the roughness height, k, is much smaller than the flow thickness h (Townsend 1976, pp. 139–143). This approximation has been the subject of controversy in recent decades (see the review by Jiménez 2004) but the evidence is now in its favour. Recent experiments and numerical simulations of rough-walled turbulent boundary layers and channels with $k/h \lesssim 0.04$ and $Re_\tau \in [400$–$5000]$ agree well with smooth-wall data (Keirsbulck *et al.* 2002; Ashafarian, Andersson & Manhart 2004; Flack, Schultz, & Shapiro 2005; Bakken *et al.* 2005; Flores & Jiménez 2006).

This evidence is hard to reconcile with a model in which the important flow structures are born near the wall. One would then expect that the organization of the outer layer would be altered by the roughness. It favours AJZM06's view that vortex clusters/packets are born at different wall-normal positions, or that clusters form at the wall, but quickly forget their origin and reach some local equilibrium with the outer layer. Either way, the importance of the wall is diminished. In this paper, we present new evidence for wall independence by comparing the vortex clusters in numerically simulated turbulent channels with smooth and rough walls.

2. Numerical experiments and cluster identification

We use data from direct numerical simulations of plane turbulent channels at $Re_\tau = u_\tau h/\nu \approx 600$, where u_τ is the friction velocity, and h is the channel half-width. The experiments are summarized in table 1, and documented comprehensively by del Álamo *et al.* (2004) and Flores & Jiménez (2006). We denote variables in wall units with a $^+$ superscript. The streamwise, wall-normal and spanwise coordinates are x, y and z, and the corresponding velocity components are u, v and w. The case labelled S has smooth walls, while the cases labelled R have harmonic velocity disturbances prescribed at the walls, which successfully mimic the effect of wall roughness by destroying the near-wall energy cycle (Flores & Jiménez 2006). The wall disturbances in R1 only have streamwise and wall-normal components, whereas those in R2

Case	Re_τ	L_x/h	L_z/h	Δx^+	Δz^+	Δy^+	k_s^+	h_R^+	α_c	N_C	N_{att}
S	547	8π	4π	13.4	6.7	6.7	–	–	0.0024	1.9×10^6	1.4×10^5
R1	632	8π	4π	11.6	5.8	8.0	129	93	0.0046	2.3×10^6	1.7×10^5
R2	674	4π	2π	12.4	6.2	8.6	207	146	0.0034	1.0×10^6	0.8×10^5

TABLE 1. Parameters of our experiments. L_x and L_z are the streamwise and spanwise dimensions of the domain and h is the channel half-height. Δx and Δz are the streamwise and spanwise collocation resolutions. Δy is the wall-normal resolution at the centreline. In cases R1 and R2, k_s is the equivalent sand roughness height and h_R is the height of the roughness sublayer, as defined by Flores & Jiménez (2006). α_c is the threshold of percolation of the vortex population, N_C is the number of extracted clusters, and N_{att} is the number of those classified as wall-attached.
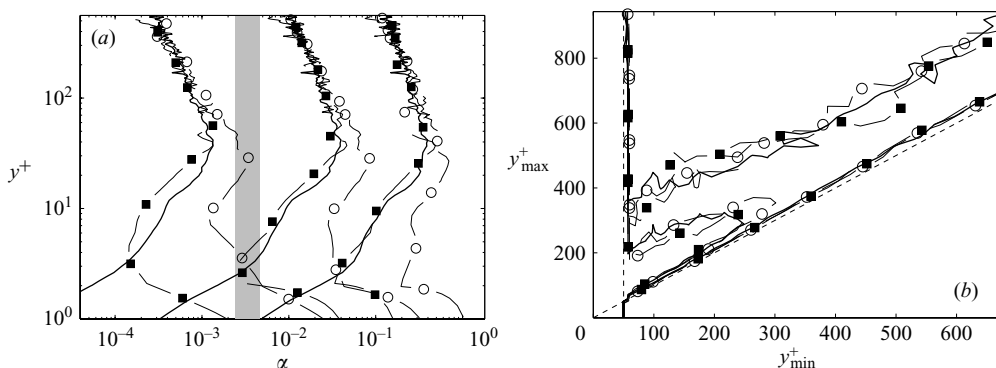

FIGURE 1. (*a*) Isolines of the relative volume V_r occupied by the points satisfying the relation (2.1) as a function of the threshold α and of the wall distance. From left to right, $V_r = 0.2, 0.04, 0.008$. The grey strip covers the range of variability of α_c for the present experiments. (*b*) Volume distribution p_V of the clusters as a function of their minimum and maximum wall distances, y_{min} and y_{max}. The levels contain 60 % and 85 % of the data. The vertical dotted line is $y_{min}^+ = 50$ and the diagonal one is $y_{min} = y_{max}$. ——, S. ○, R1. ■, R2.

are three-dimensional. In addition, the streamwise wavelength of the forcing in R1 ($\Lambda_x^+ = 220$) is shorter than in R2 ($\Lambda_x^+ = 529$). As a consequence, the equivalent sand roughness height and the thickness h_R of the roughness sublayer are larger in R2 than in R1. The spanwise wavelength of the forcing is $\Lambda_z = \Lambda_x/2$ in both cases.

We employ the method described by AJZM06 to extract $O(10^6)$ vortex clusters from instantaneous flow realizations (see table 1). They are defined as sets of connected points where the discriminant D of the velocity gradient tensor is larger than a certain fraction of its standard deviation σ_D in the wall-parallel plane,

$$D > \alpha\sigma_D(y). \qquad (2.1)$$

Figure 1(*a*) shows the relative volume V_r occupied by the clusters as a function of the threshold α, and of the wall distance. The three flows agree fairly well above the roughness sublayer, $y^+ > 100 \approx h_R^+$, but differ appreciably below that level, especially for $y^+ \leqslant 50$. These discrepancies lead to different connectivities in the roughness sublayer which affect all the wall-attached objects, including the interesting ones reaching into the logarithmic and outer layers. We therefore apply our cluster

identification algorithm to the truncated domain $50 < y^+ < 2Re_\tau - 50$ for the three flows in table 1, which allows us to compare consistently the clusters from the rough- and the smooth-walled cases. The results obtained from full channels, and from channels truncated at other wall distances, agree qualitatively with those presented below.

In our analysis, we use $\alpha = 0.0055 \approx \alpha_c$, where α_c is the critical threshold below which a cluster percolates throughout the truncated channel (see table 1). The percolation thresholds from cases S, R1 and R2 differ little from one another, taking into account that α multiplies a sixth power of the vorticity. This is emphasized by the narrowness of the grey bar representing the range of variability of α_c in figure 1(*a*). Our value of α is closer to the percolation threshold than those used by AJZM06, because only when $\alpha \approx \alpha_c$ does the vortex distribution become independent of Re_τ in the outer region. This allows us to compare the results from S, R1 and R2 despite their different Reynolds numbers. The results for other values of α are very similar (Flores 2007).

Figure 1(*b*) shows isocontours of the distribution of volume occupied by the clusters as a function of the minimum and maximum wall distances of these objects, $p_V(y_{min}, y_{max})$. Similar to the smooth-wall cases reported by AJZM06, the shape of p_V suggests that the population of clusters in rough-walled channels may be divided into *wall-detached* and *wall-attached* families. The wall-detached family is the wide inclined strip where the volume distribution is approximately homogeneous, $p_V \approx p_V(y_{max} - y_{min})$, and is formed by clusters that reside away from the wall. The wall-attached family is the thin vertical strip formed by clusters whose minimum wall distance coincides with the boundary of the truncated-height channel, $y_{min}^+ = 50$.

Because our definition of an attached cluster is slightly different from that in AJZM06 ($y_{min}^+ < 20$), we classify as attached some objects that they would have classified as detached. However, the differences are small, especially for large clusters reaching the outer region. The analysis of $p_V(y_{min}, y_{max})$ in full channels (plotted in AJZM06) shows that 25 % of the clusters in S with $y_{max}^+ = 100$, and 10 % of those with $y_{max}^+ = 200$, switch families between the two definitions. These figures only represent 6 % of the total cluster population. Similar results are obtained for cases R1 and R2.

In the rest of this paper, we analyse the wall-attached clusters to evaluate the possibility of inner–outer interactions caused by vortex loops emanating from the buffer layer. We focus on them because they are important for the dynamics of the outer region (AJZM06), and because they could be argued to depend on the details of the wall, due to their wall-attached nature. The detached clusters are just dissipative eddies and, as expected, are not affected by the wall (for more details see AJZM06 and Flores 2007).

3. The geometry and distribution of the attached clusters

Figure 2(*a*) shows joint p.d.f.s of the streamwise and wall-normal sizes of the attached clusters (Δ_x, Δ_y), defined as those of the Cartesian boxes that circumscribe them. In AJZM06, the attached clusters had $y_{min}^+ < 20$, and $\Delta_y = y_{max} - y_{min}$ and y_{max} were roughly equal. In our case, the minimum wall distance of the attached clusters very likely lies below the truncation level, $y_{min}^+ = 50$. Since this cutoff can be an appreciable fraction of the cluster height, y_{max} seems a better measure of that height than Δ_y. However, we use Δ_y in figure 2(*a*) because the length of the cluster Δ_x is only measured above $y_{min}^+ = 50$.

In the preparation of the figure, clusters with vortex volumes smaller than 30^3 wall units have not been considered because their sizes are of the order of the simulation
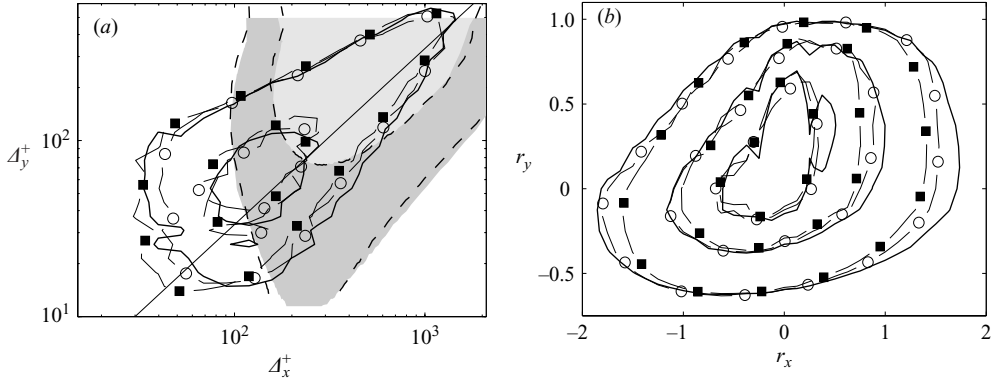
FIGURE 2. (*a*) Isolines of the joint p.d.f.s of the logarithms of the length and the height of the attached clusters $p(\Delta_x^+, \Delta_y^+)$, containing 40 % and 94 % of the data. The shaded patches are contours of the premultiplied spectral density $\phi_{vv}(\lambda_x, y - y_{min})$ of v^2 from case S, while the dashed lines correspond ϕ_{vv} from case R1. We have plotted the levels 1/4 and 1/2 times the maximum of ϕ_{vv}, using the correspondence $\lambda \sim \Delta$. The straight solid line is (3.1). (*b*) P.d.f. of the relative positions of the vortex cores in the circumscribing boxes of the attached clusters with $y_{max}^+ > 100$. The contours contain 20 %, 50 % and 80 % of the data. ——, S. ○, R1. ■, R2.

grid. The results show that the distributions of sizes of the attached clusters do not depend on the wall forcing, with the exception of the clusters that are fully contained in the roughness sublayer of channels R1 and R2 ($\Delta_y^+ \lesssim 50$). Even in that case, the size of the clusters is not set by the wavelength of the forcing. Similar results are obtained for $p(\Delta_z^+, \Delta_y^+)$ and $p(\Delta_x^+, \Delta_z^+)$, not shown here. In all of these distributions, the clusters from our three flows show the self-similar scalings reported by AJZM06,

$$\Delta_x \approx 3\Delta_y, \quad \Delta_x \approx 2\Delta_z. \tag{3.1}$$

Figure 2(*a*) also includes the spectral energy densities of v for S (shaded) and R1 (dashed lines), as functions of $y - y_{min}$, showing the good agreement between the rough- and the smooth-walled cases. Furthermore, the most energetic scales coincide reasonably well with the cluster sizes, consistent with the idea that the attached clusters are markers for wall-normal velocity structures. Notice that this conclusion is not invalidated by the imperfect agreement in figure 2(*a*), because the correspondence between wall distance and cluster height is only approximate, and because sizes are proportional but not equal to spectral wavelengths (Jiménez, del Álamo & Flores 2004).

The average shape of the tall attached clusters is shown in figure 2(*b*), which presents p.d.f.s of the coordinates of the points belonging to each cluster, with respect to the centre, x_c, z_c, and $y_c = y_{max}/2$, of its circumscribing box. The scaled position vector in that reference frame is defined as $\boldsymbol{r} = (\boldsymbol{x} - \boldsymbol{x}_c)/y_c$. The results show that the p.d.f.s of (r_x, r_y) depend little on the nature of the wall. The slight discrepancy observed for the outer contour at $|r_x| \approx 1$ shows that the attached clusters are slightly more elongated in the smooth- than in the rough-walled channel. The observed differences disappear when larger clusters are considered, or when the channel is truncated at $y_{min}^+ = 100$, which suggests that these differences are caused by the lower mean shear near the rough walls, rather than by the direct effect of the wall disturbances. This is confirmed because the transverse p.d.f.s of (r_x, r_z) and (r_z, r_y), which are not affected by the shear, agree perfectly for the smooth- and rough-walled cases (not shown).
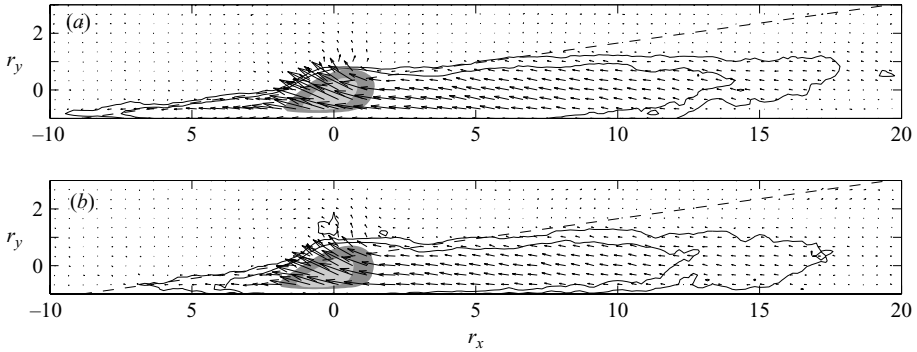
FIGURE 3. Quiver plot of the average fluctuating velocity field ($\langle u' \rangle$, $\langle v' \rangle$) conditioned to the presence of tall attached clusters ($y^+_{max} > 200$). The data are taken at the plane $r_z = 0$. The contour lines are $\langle u' \rangle^+ = -0.05, -0.1$. The shaded contours contain 33 % and 66 % of the p.d.f. of the positions of points inside the conditioning clusters. The dashed lines have a slope of 8°. (*a*) S, longest arrow $0.93u_\tau$. (*b*) R1, longest arrow $0.81u_\tau$.

The results presented in figure 2 indicate that the sizes and shapes of the attached clusters are not affected by the nature of the wall. Flores (2007) shows that this is also true for other cluster properties, such as the fraction of Reynolds stresses contained in their circumscribing boxes, or their volume density per unit wall distance. These results suggest that the attached clusters are either generated away from the wall, or that they forget their origin soon after they are born. Note that the two possibilities do not exclude each other: the lifetimes of the wall-normal velocity reported by AJZM06 support the first, while the analysis by Flores & Jiménez (2007) of the linear evolution of concentrated perturbations in a logarithmic layer supports the second.

4. The average velocity field conditioned to the tall attached clusters

We mentioned in the introduction that the conditionally averaged flow field in the neighbourhood of the attached clusters contains a lambda-vortex and a *v*-ejection. AJZM06 showed that, in smooth channels, it also anchors a conical low-*u* structure that was too long to be contained within their averaging box, but that was at least 10 times longer than the conditioning cluster. In this section, we analyse the effect of wall roughness on those structures. We have excluded data from R2, whose box length is marginally too short for that purpose, even though its conditionally averaged fields are in qualitative agreement with those below.

We define the average velocity fluctuations conditioned to a cluster set as

$$\langle \boldsymbol{u}' \rangle (\boldsymbol{r}) = \sum_{i}^{N} \boldsymbol{u}'(\boldsymbol{x}_{c,i} + y_{c,i}\boldsymbol{r})y_{c,i}^3 \bigg/ \sum_{i}^{N} y_{c,i}^3, \qquad (4.1)$$

where the prime denotes fluctuations with respect to the mean velocity profile, and the subindex *i* refers of the *i*th cluster of the set. As in AJZM06, the weight factor $y_{c,i}^3$ ensures that (4.1) is an unbiased ensemble average, since the probability of sampling a given structure is proportional to its volume. Figure 3 shows $\langle \boldsymbol{u}' \rangle (r_z = 0)$ for tall attached clusters, defined here as those with $y^+_{max} > 200$. The results from the two cases are nearly identical, and similar to the conical wakes obtained by AJZM06 at higher Reynolds numbers. The main difference is that the upstream (left) part of the wake is shorter for R1, probably due to the lower mean shear of this flow below $y^+ \approx 100$.
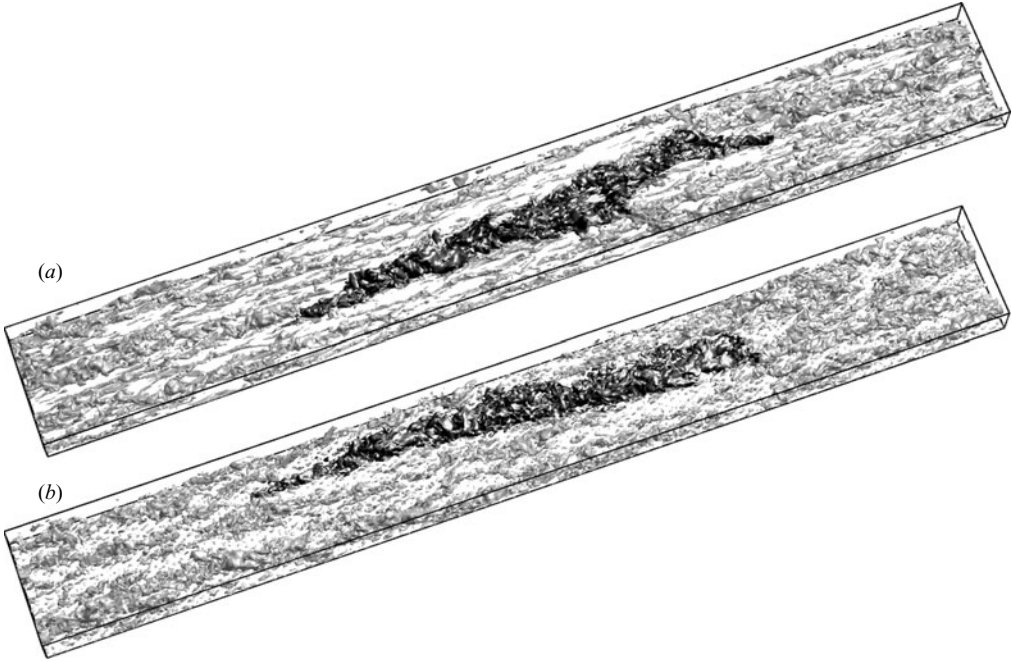
FIGURE 4. Snapshots of the surface $u'^+ = -2$ in cases S (*a*) and R1 (*b*). The flow goes from left to right. The size of the plotted boxes is $8\pi h \times \pi h \times h$. Two large structures similar to the $u' < 0$ cones in figure 3 have been manually highlighted in black.

The slope of the u-structures in figures 3(*a*) and 3(*b*) is approximately equal to $8°$ for $-2 < r_x < 5$. It decreases beyond $r_x \approx 5$, and the low-speed cones level off to $r_y \approx 1.5$, and to a width $r_z \approx \pm 1$ for $r_x \gtrsim 8$. We can estimate the size of a typical, tall attached cluster as the mean of the distribution $p_V(y_{\min}^+ = 50, y_{\max}^+ > 200)$, which is $y_{\max}^+ \approx 400$. For this typical cluster, the saturation height and width of the low-u wake in figure 3 would be approximately $500\nu/u_\tau$. Cross-flow visualizations (see Flores 2007, or AJZM06) show that the low-u wake is flanked by weaker high-speed regions, resulting in a spanwise wavelength $\lambda_z^+ \approx 900$.

This saturation is probably due to the limited Reynolds number of our simulations, and it was not observed by AJZM06. They used a somewhat higher threshold to identify vortices, a lower near-wall cutoff, and a higher Reynolds number. As a consequence, their cluster population was dominated by smaller objects with respect to the channel height, and the levelling-off was not observed within their averaging box. Note that the coordinates in figure 3 are scaled with the size of the conditioning cluster.

In the present case, the levelling-off occurs at cross-stream dimensions of the order of the channel half-width, which agree well with the spectral wavelengths of the global modes identified by Bullock, Cooper & Abernathy (1978) and del Álamo & Jiménez (2003) over smooth walls, and by Flores & Jiménez (2006) and Metzger, McKeon & Holmes (2007) over rough ones. The length of the cylindrical sections in figure 3 is about $x/h \approx 3$–7, which corresponds to the shorter end of these global modes. Del Álamo *et al.* (2004) had already concluded that the widest modes in the spectra of u were determined by the saturation in the growth of the u-structures when they reach diameters comparable to the channel height.

The connection between figure 3 and the global modes is confirmed by instantaneous flow visualizations. Figure 4 shows three-dimensional representations of the surface
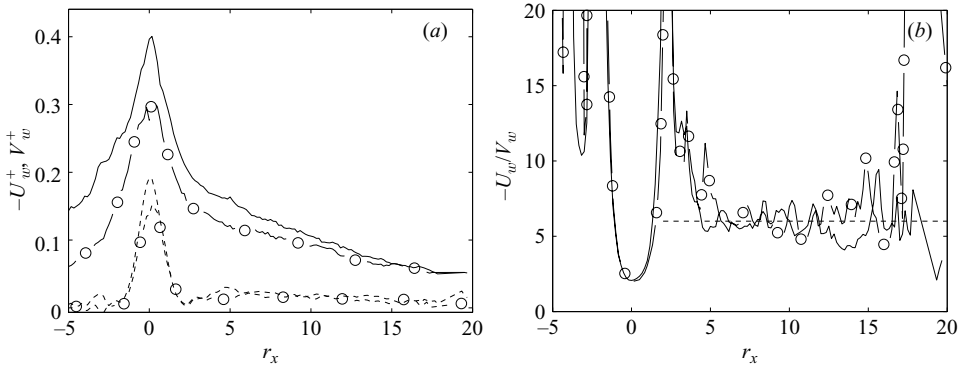
FIGURE 5. Mean velocity fluctuations inside the cone, U_w and V_w (see (4.2)), for attached clusters with $y_{max}^+ > 200$. (a) Velocities in wall units, solid lines correspond to $-U_w^+$ and dashed lines to V_w^+. (b) Ratio $-U_w/V_w$, the horizontal line is $-U_w/V_w = 6$. ——, S. ○, R1.

$u'^+ = -2$ in sub-domains of S and R1. A large conical structure, reminiscent of the averaged velocity fields in figure 3, has been highlighted near the centre of each plot. Although the details of the highlighting are arbitrary in that both structures could be continued into much longer roughly cylindrical streaks, the identification of the initial conical part is in each case essentially unambiguous. The longer downstream structures attached to these regions have lengths of the same order as the simulation box, and recall the very long u-structures identified over smooth (Kim & Adrian 1999; del Álamo *et al.* 2004; Hutchins & Marusic 2007) and rough (Flores & Jiménez 2006) walls. Note that the near-wall streaks are clearly visible in case S, but in R1 they have been substituted by a regular array of spots generated by the wall disturbances. Similar structures are found in all the instantaneous realizations that were inspected. The only manipulation in the figure has been to centre them in the display box.

It was shown by Flores & Jiménez (2006) that the global modes are very efficient in generating Reynolds stresses, because their wall-normal and spanwise velocity components are highly correlated. The same happens with the saturated part of the cones shown in figure 3. We define the mean velocity fluctuations inside the cones as

$$U_w(r_x) = A_\Omega^{-1} \int_{\Omega(r_x)} \langle u' \rangle \, \mathrm{d}A, \quad V_w(r_x) = A_\Omega^{-1} \int_{\Omega(r_x)} \langle v' \rangle \, \mathrm{d}A, \qquad (4.2)$$

where $\Omega(r_x)$ is the region where $\langle u' \rangle^+ < -0.05$ at each streamwise location. These velocities are shown in figure 5(a) for clusters with $y_{max}^+ > 200$. Both U_w^+ and V_w^+ peak at the centre of the cluster but the mean fluctuating velocities from case R1 are somewhat weaker than those from case S. This agrees with Flores & Jiménez (2006), who found that the global modes were slightly stronger over smooth than over rough walls, and attributed that difference to the lower centreline velocity of the latter.

Figure 5(b) shows that the ratio U_w/V_w, which is a measure of the efficiency of v in creating u-perturbations from the mean velocity profile, is reasonably constant in the range $5 < r_x < 15$. The level of the plateau is higher than the overall ratio of the r.m.s. turbulent intensity in the outer layer $\overline{(u'^2)}/\overline{(v'^2)} \approx 1.5$–2 (the overline denotes time and wall-parallel averaging). The level in figure 5(b) is of the same order as the structure parameter for the Reynolds stresses $-\overline{(u'^2)}^{1/2}/\overline{(u'v')}^{1/2} \approx 4.5$–5, which measures only the part of v correlated with u. It is also of the order of the ratio between the energy spectrum of the streamwise velocity and the Reynolds-stress cospectrum, which is

$-\phi_{uu}/\phi_{uv} \approx 3$–$7$ for wavelengths of the order of $5h \times h$, outside the buffer layer. These figures are consistent with the interpretation of the saturated parts of the structures in figure 3 as global modes. Other values of the threshold in the definition of $\Omega(r_x)$, and any reasonable range of sizes for the attached clusters with $y_{\max}^+ > 100$, lead to the same plateau as in figure 5(*b*).

5. Conclusions

We have investigated the vortex clusters found in turbulent channels with rough walls at moderate Reynolds numbers. As in the smooth-walled case, they separate into wall-attached and wall-detached families. We have payed special attention to those attached clusters that reach above the roughness sublayer and into the outer region of the flow. They play an important role in the dynamics of the turbulent outer layer (AJZM06), and have many characteristics in common with the constitutive elements of a number of models that represent that part of the flow by hierarchies of vortex loops emanating from the wall (Perry & Chong 1982; Perry & Marusic 1995).

Our results indicate that the geometry and spatial distribution of the attached clusters are independent of the details of the wall. These clusters are associated with cones of negative streamwise velocity fluctuations both over smooth and over rough walls. The only appreciable effects of the wall details are restricted to the roughness sublayer, where the lower mean shear of the rough-walled flows leads to shorter cones.

These observations, together with the lifetimes obtained by AJZM06 for the structures in channels at higher Re_τ, suggest that either the clusters are generated at all heights, or that they quickly become self-similar and forget their origin. The present results help to reconcile the attached-eddy models with Townsend's hypothesis that the outer layer is independent of the wall details, which is receiving increased support (Keirsbulck *et al.* 2002; Flack *et al.* 2005; Bakken *et al.* 2005; Flores & Jiménez 2006).

Finally, we have shown that the cones level off when their widths and heights become of the order of the channel half-height. These parts of the structures are the global modes identified by del Álamo *et al.* (2004), and the analysis of their mean streamwise and wall-normal velocity fluctuations shows that their wall-normal and streamwise velocity components are highly correlated, in agreement with del Álamo & Jiménez (2003) and Flores & Jiménez (2006).

REFERENCES

ADRIAN, R. J., MEINHART, C. D. & TOMKINS, C. D. 2000 Vortex organization in the outer region of the turbulent boundary layer. *J. Fluid Mech.* **422**, 1–53.

DEL ÁLAMO, J. C. & JIMÉNEZ, J. 2003 Spectra of the very large anisotropic scales in turbulent channels. *Phys. Fluids* **15**, L41–L44.

DEL ÁLAMO, J. C., JIMÉNEZ, J., ZANDONADE, P. & MOSER, R. D. 2004 Scaling of the energy spectra of turbulent channels. *J. Fluid Mech.* **500**, 135–144.

DEL ÁLAMO, J. C., JIMÉNEZ, J., ZANDONADE, P. & MOSER, R. D. 2006 Self-similar vortex clusters in the logarithmic region. *J. Fluid Mech.* **561**, 329–358.

ASHAFARIAN, A., ANDERSSON, H. I. & MANHART, M. 2004 DNS of turbulent flow in a rod-roughened channel. *Intl J. Fluid Flow* **25**, 373–383.

BAKKEN, O. M., KROGSTAD, P. A., ASHFARIAN, A. & ANDERSSON, H. I. 2005 Reynolds number effects in the outer layer of the turbulent flow in a channel with rough walls. *Phys. Fluids* **17**, 065101.

BLACKBURN, H. M., MANSOUR, N. N. & CANTWELL, B. J. 1996 Topology of fine-scale motions in turbulent channel flow. *J. Fluid Mech.* **310**, 269–292.

BULLOCK, K. J., COOPER, R. E. & ABERNATHY, F. H. 1978 Structural similarity in radial correlations and spectra of longitudinal velocity fluctuations in pipe flow. *J. Fluid Mech.* **88**, 585–608.

CHONG, M. S., SORIA, J., PERRY, A. E., CHACIN, J., CANTWELL, B. J. & NA, Y. 1998 Turbulence structures of wall-bounded flows using DNS data. *J. Fluid Mech.* **357**, 225–247.

FLACK, K. A., SCHULTZ, M. P. & SHAPIRO, T. A. 2005 Experimental support for Townsend's Reynolds number similarity hypothesis on rough walls. *Phys. Fluids* **17**, 035102.

FLORES, O. 2007 The dynamics of the outer region of wall-bounded turbulence. PhD thesis, Universidad Politécnica de Madrid, in preparation.

FLORES, O. & JIMÉNEZ, J. 2006 Effect of wall-boundary disturbances on turbulent channel flows. *J. Fluid Mech.* **566**, 357–376.

FLORES, O. & JIMÉNEZ, J. 2007 Linear dynamics of self-similar structures in the turbulent logarithmic region. *J. Fluid Mech.* (submitted).

GANAPATHISUBRAMANI, B., LONGMIRE, E. K. & MARUSIC, I. 2003 Characteristics of vortex packets in turbulent boundary layers. *J. Fluid Mech.* **478**, 35–46.

HUTCHINS, N. & MARUSIC, I. 2007 Evidence of very long meandering features in the logarithmic region of turbulent boundary layers. *J. Fluid Mech.* **579**, 1–28.

JIMÉNEZ, J. 2004 Turbulent flows over rough walls. *Annu. Rev. Fluid Mech.* **36**, 173–196.

JIMÉNEZ, J., DEL ÁLAMO, J. C. & FLORES, O. 2004 The large-scale dynamics of near-wall turbulence. *J. Fluid Mech.* **505**, 179–199.

KEIRSBULCK, L., LABRAGA, L., MAZOUZ, A. & TOURNIER, C. 2002 Surface roughness effects on turbulent boundary layer structures. *Trans. ASME: J. Fluids Engng* **124**, 127–135.

KIM, K. & ADRIAN, R. J. 1999 Very large-scale motion in the outer layer. *Phys. Fluids* **11**, 417–422.

METZGER, M., MCKEON, B. J. & HOLMES, H. 2007 The near-neutral atmospheric surface layer: turbulence and non-stationarity. *Phil. Trans. R. Soc. Lond.* A **365**, 859–876.

PERRY, A. E. & CHONG, M. S. 1982 On the mechanism of wall turbulence. *J. Fluid Mech.* **119**, 173–217.

PERRY, A. E., HENBEST, S. & CHONG, M. S. 1986 A theoretical and experimental study of wall turbulence. *J. Fluid Mech.* **119**, 163–199.

PERRY, A. E. & MARUSIC, I. 1995 A wall-wake model for the turbulence structure of boundary layers. 1. Extension of the attached eddy hypothesis. *J. Fluid Mech.* **298**, 361–388.

ROBINSON, S. K. 1991a Coherent motions in the turbulent boundary layer. *Annu. Rev. Fluid Mech.* **23**, 601–639.

ROBINSON, S. K. 1991b The kinematics of turbulent boundary layer structure. PhD thesis, NASA Ames Research Center.

TANAHASHI, M., KANG, S.-J., MIYAMOTO, T., SHIOKAWA, S. & MIYAUCHI, T. 2004 Scaling of fine scale eddies in turbulent channel flows up to $Re_\tau = 800$. *Intl J. Heat Fluid Flow* **25**, 331–340.

TOMKINS, C. D. & ADRIAN, R. J. 2003 Spanwise structure and scale growth in turbulent boundary layers. *J. Fluid Mech.* **490**, 37–74.

TOWNSEND, A. A. 1976 *The Structure of Turbulent Shear Flows*, 2nd edn. Cambridge University Press.

ZHOU, J., ADRIAN, R. J., BALACHANDAR, S. & KENDALL, T. M. 1999 Mechanisms for generating coherent packets of hairpin vortices in channel flow. *J. Fluid Mech.* **387**, 353–396.